Glycerol-3-phosphate Acyltransferase Isoform-4 (GPAT4) Limits Oxidation of Exogenous Fatty Acids in Brown Adipocytes[*]

Daniel E. Cooper[‡], Trisha J. Grevengoed[‡], Eric L. Klett[‡§], and Rosalind A. Coleman[‡1]

From the Departments of [‡]Nutrition and [§]Medicine, University of North Carolina, Chapel Hill, North Carolina 27599

Background: GPAT4 is a major glycerol-3-phosphate acyltransferase (GPAT) isoform in brown adipose tissue (BAT).
Results: Compared with control cells, brown adipocytes lacking GPAT4 oxidize 40% more exogenous fatty acids.
Conclusion: GPAT4 in BAT is required to limit oxidation of exogenous fatty acid.
Significance: The function of each GPAT isoform is tissue-specific and evolved to perform a unique function within a physiological context.

Glycerol-3-phosphate acyltransferase-4 (GPAT4) null pups grew poorly during the suckling period and, as adults, were protected from high fat diet-induced obesity. To determine why $Gpat4^{-/-}$ mice failed to gain weight during these two periods of high fat feeding, we examined energy metabolism. Compared with controls, the metabolic rate of $Gpat4^{-/-}$ mice fed a 45% fat diet was 12% higher. Core body temperature was 1 °C higher after high fat feeding. Food intake, fat absorption, and activity were similar in both genotypes. Impaired weight gain in $Gpat4^{-/-}$ mice did not result from increased heat loss, because both cold tolerance and response to a β3-adrenergic agonist were similar in both genotypes. Because GPAT4 comprises 65% of the total GPAT activity in brown adipose tissue (BAT), we characterized BAT function. A 45% fat diet increased the $Gpat4^{-/-}$ BAT expression of peroxisome proliferator-activated receptor α (PPAR) target genes, $Cpt1\alpha$, $Pgc1\alpha$, and $Ucp1$, and BAT mitochondria oxidized oleate and pyruvate at higher rates than controls, suggesting that fatty acid signaling and flux through the TCA cycle were enhanced. To assess the role of GPAT4 directly, neonatal BAT preadipocytes were differentiated to adipocytes. Compared with controls, $Gpat4^{-/-}$ brown adipocytes incorporated 33% less fatty acid into triacylglycerol and 46% more into the pathway of β-oxidation. The increased oxidation rate was due solely to an increase in the oxidation of exogenous fatty acids. These data suggest that in the absence of cold exposure, GPAT4 limits excessive fatty acid oxidation and the detrimental induction of a hypermetabolic state.

Glycerol-3-phosphate acyltransferase (GPAT)[2] (EC 2.3.1.15) catalyzes the esterification of long-chain acyl-CoAs at the sn-1 position of glycerol-3-P and is the initial and rate-limiting step for the synthesis of triacylglycerol (TAG) and all the glycerophospholipids. Four mammalian GPAT isoforms, each the product of a separate gene, have been identified, and the phenotypes differ in mice deficient in GPAT1, -3, and -4. Lack of GPAT1 results in lower hepatic TAG content with less palmitate in the sn-1 position of phosphatidylcholine and phosphatidylethanolamine, resistance to high fat diet (HFD; 45% fat diet)-induced insulin resistance (1, 2), increased hepatic fatty acid oxidation (1), and resistance to diethylnitrosamine-induced hepatocellular carcinoma (3). GPAT3 contributes nearly 80% of total GPAT activity in white adipose tissue, but GPAT3-deficient mice are not lipodystrophic and gain weight normally when fed a high fat diet (4, 5). A mouse deficient in GPAT2 has not been reported, and recent data suggest that GPAT2 may esterify both glycerol-3-P and lysoglycerol-3-P in testis (6). Many of the phenotypic differences in GPAT-null animals are likely due to a variation in nutritional regulation and tissue-dependent expression of each GPAT isoform.

Previously called acylglycerol-3-phosphate acyltransferase isoform 6 (AGPAT6) because of its similarity to AGPAT1 and -2, GPAT4 has 66% amino acid identity to GPAT3 and does not possess AGPAT activity (7). GPAT4 is a major GPAT isoform in liver (8) and is highly expressed in the mammary gland where it is required for development and for the deposition of diacylglycerol and TAG in milk (9). In $Gpat4^{-/-}$ liver, compared with controls, total GPAT specific activity and TAG content are 45% lower (7, 10). Mice deficient in GPAT4 are protected from diet and genetically induced obesity, and, compared with controls, their metabolic rate was reported to be 5% higher (5). This metabolic phenotype had been attributed to the absence of a subdermal adipose layer at 12 weeks of age (7). However, it is unclear whether the lack of subdermal adipose in $Gpat4^{-/-}$ mice is the cause of or an adaptation to the higher metabolic rate.

To determine whether $Gpat4^{-/-}$ mice are resistant to adipose tissue accumulation because of a broader influence on energy metabolism and to investigate the mechanism whereby GPAT4-deficient mice are protected from obesity, we characterized the growth and weight gain of littermate control and

[2] The abbreviations used are: GPAT, glycerol-3-phosphate acyltransferase; HFD, high fat diet; TAG, triacylglycerol; NEM, N-ethylmaleimide; BAT, brown adipose tissue; ASM, acid-soluble metabolites; FA, fatty acid; PPAR, peroxisome proliferator-activated receptor.

Gpat4^{−/−} mice from birth to 8 weeks of age. Additionally, we evaluated the metabolic changes in female mice after a 4-week 45% fat diet challenge. These studies enabled us to evaluate metabolic changes associated with a shift in dietary substrate before the onset of obesity, and indicated that the mice were hypermetabolic and had excess FA use in brown adipose tissue. Although GPAT4 comprises 65% of the total GPAT activity in BAT, its role in this tissue had not been investigated (8). Our studies provide evidence that the lack of GPAT4 protects mice from obesity because GPAT4 normally limits the oxidation of exogenously provided FA by brown adipocytes.

Experimental Procedures

Materials—Type I collagenase was from Worthington Biochemical Corporation. [2-^{14}C]Pyruvic acid, [1-^{14}C]oleic acid, and [9,10-^{3}H]oleic acid were purchased from PerkinElmer Life Sciences. Silica Gel G plates were from Whatman. Tissue culture plates were from BD Biosciences, and media were obtained from Invitrogen. Sigma was the source of all other chemicals, unless otherwise indicated.

Animal Care—Animal protocols were approved by the University of North Carolina at Chapel Hill Institutional Animal Care and Use Committee. Mice were housed in a pathogen-free barrier facility on a 12-h light/dark cycle with free access to water and food (Prolab 5P76 Isopro 3000; 5.4% fat by weight). *Gpat4*^{−/−} mice were backcrossed at least eight times onto a C57BL6/J background. *Gpat4*^{−/−} mice were compared with littermate controls, all born to heterozygous dams because homozygous females produce milk that is deficient in TAG (5). Male and female mice had similar phenotypes. Unless noted in the figure legends, female mice were used. At 8 weeks of age, littermate controls and *Gpat4*^{−/−} mice were either fed a control diet containing 10% kcal from fat or a matched high fat diet containing 45% kcal from fat, for either 4 or 8 weeks (Research Diets D12450H and D12451, respectively). Body weights were measured weekly. Using a BAT10 thermometer with rectal probe attachment (Physitemp Instruments, Inc.), rectal temperature was measured between 10 a.m. and 12 p.m. To determine fecal TAG content, control and *Gpat4*^{−/−} mice of both sexes were housed individually and fed a diet containing 60% kcal from fat (Research Diets, D12452). Before collection of blood or tissues, food was removed from mouse cages for 4 h, and mice were anesthetized with 250 mg/kg of Avertin unless otherwise stated. Body composition was determined with a 7T Bruker PharmaScan MRI system (Bruker BioSpin Corporation). After the MRI, mice were placed in individual TSE Lab Systems metabolic cages (TSE Systems International Group) for 72 h to measure metabolic performance by indirect calorimetry. To allow mice to acclimate, data were collected after the first 24 h in the metabolic cages. Using the Weir equation $(REE = [3.9(VO_2) + 1.1(VCO_2)]1.44)$, energy expenditure was calculated and normalized to the lean body mass of each mouse. Before cold tolerance tests, 12-week-old control and *Gpat4*^{−/−} mice fed a 10% fat diet for 4 weeks were fasted for 4 h. Mice were placed into individual cages without food or bedding in a 4 °C cold room. Rectal temperatures were measured at 0, 1, 2, 3, and 4 h. To measure VO_2 in response to β-adrenergic stimulation, 12-week-old control and *Gpat4*^{−/−} mice fed a 10% fat diet for 4

weeks were placed into metabolic cages (TSE Systems International Group). Mice were transferred to TSE cages at 7 a.m. and acclimated until 10 a.m. Baseline O_2 consumption measurements were collected from 10 a.m. to 1 p.m. Mice were injected intraperitoneally with 5 mg/kg of CL316243 at 1 p.m. with measurements collected until 4 p.m.

GPAT Activity—After the diet challenge, tissues from control and *Gpat4*^{−/−} mice were excised and frozen in liquid N_2, and stored at −80 °C until further use. To obtain intestinal mucosa, intestines were resected, flushed with ice-cold phosphate-buffered saline (PBS), divided into four equal sections, and longitudinally dissected to expose the mucosa that was scraped using a clean microscope slide. One hundred milligrams of tissue was homogenized in ice-cold Medium I buffer (250 mM sucrose, 10 mM Tris, pH 7.4, 1 mM EDTA, 1 mM dithiothreitol) using 10 up-and-down strokes of a Potter-Elvehjem homogenizer. Total membranes were isolated by centrifuging the homogenate at $100,000 \times g$ for 1 h. GPAT initial rates were measured with 800 μM [^{3}H]glycerol 3-phosphate, and 82.5 μM palmitoyl-CoA (11). The reaction was initiated by adding 10 (cells) or 5–50 μg (tissue) of membrane protein after incubating the membrane protein on ice for 15 min in the presence or absence of 2 mM *N*-ethylmaleimide (NEM), which inactivates GPAT isoforms 2, 3, and 4. The reaction products were extracted into $CHCl_3$, dried under N_2, resuspended in 4 ml of Cytoscint, and counted in a scintillation counter. NEM-resistant activity (GPAT1) was calculated by subtracting NEM-sensitive activity from total activity.

Measurement of Acute Lipid Absorption—Twelve-week-old control and *Gpat4*^{−/−} mice were fasted for 4 h, and anesthetized with isoflurane gas, after which 200 μl of 15% Tyloxapol was injected into the retroorbital plexus to inhibit lipoprotein lipase activity and prevent TAG clearance by peripheral tissues (12). Fifteen minutes after the Tyloxapol injection, blood was collected for baseline TAG measurement, and mice were gavaged with 200 μl of olive oil. Blood was collected via tail nick at 1, 2, 4, and 6 h after gavage. Plasma TAG was measured colorimetrically (Stanbio).

Lipid Extraction and TAG Measurement in Feces and Brown Adipose Tissue and Cells—Feces were collected, pulverized under liquid nitrogen, and extracted by the Folch method (13). Lysates from brown adipose and primary brown adipocytes were extracted similarly. Chloroform extracts were dried under N_2 gas and resuspended in 200 μl of *tert*-butanol:methanol:Triton X-100 (3:1:1, v/v/v). TAG was determined as described above.

Osmium Tetroxide Staining in Small Intestine—The small intestine was resected, flushed with ice-cold PBS, and divided into 3 equal sections. Sections were fixed in 1.5% glutaraldehyde, neutral lipids were stained in 2% osmium tetroxide (14), and visualized using light microscopy.

2-Br-[1-^{14}C]palmitate and 2-Deoxy[1-^{14}C]glucose Uptake—To determine 2-Br-[1-^{14}C]palmitate uptake, anesthetized mice were injected retroorbitally with 200 μl of 1% FA-free BSA solution containing 2 μCi of 2-Br-[1-^{14}C]palmitate. To determine 2-deoxy[1-^{14}C]glucose uptake, 200 μl of sterile PBS containing 2 μCi of 2-deoxy[1-^{14}C]glucose was injected intraperitoneally. For both experiments, blood was collected via tail nick 5 min

after injection. Thirty minutes after injection, tissues were excised, weights were recorded, and tissues were snap frozen in liquid N_2. Tissues were homogenized in 1 ml of water with a blade homogenizer. Aliquots of 250 μl of tissue homogenates and 3 ml of Ecolite were mixed in scintillation vials with radioactivity counted by a scintillation counter. All measurements were performed in duplicate, and data were expressed as DPM/g tissue/DPM in 5 μl of plasma 5 min after injection/30 min.

RNA Extraction and RT-PCR—Extraction of total RNA, cDNA synthesis, and RT-PCR were performed using primer sequences and data normalization as described (15).

Mitochondrial Isolation, and Fatty Acid and Pyruvate Oxidation—BAT from control and *Gpat4$^{-/-}$* mice fed a 45% fat diet were excised, and mitochondria were isolated (15) and resuspended in mitochondrial isolation buffer containing 1 mM EDTA, 250 mM sucrose, 10 mM Tris-HCl, pH 7.8, and Complete protease inhibitor (Roche Biosciences). Forty micrograms of mitochondrial protein was incubated at 37 °C with 200 μM [1-^{14}C]oleic acid or [2-^{14}C]pyruvic acid in a sealed tube. The use of [2-^{14}C]pyruvate (rather than [1-^{14}C]) permits the measurement of CO_2 release after a complete cycle through the TCA cycle. After 30 min, the reaction was stopped with 100 μl of 70% perchloric acid and CO_2 was liberated. CO_2 was trapped in 250-μl microcentrifuge tubes containing 1 M NaOH by incubating the tubes at room temperature for 1 h with shaking. The acidified media were incubated overnight with 15% BSA and then centrifuged at 14,000 × g for 20 min. Aliquots of the supernatant were counted for radiolabeled acid-soluble metabolites (ASM), a measure of incomplete FA oxidation.

[1-^{14}C]Oleate and [9,10-^{3}H]Oleate Incorporation, Oxidation, and Lipid Extraction in Primary Brown Adipocytes—Primary brown adipocyte precursors were isolated, cultured, and differentiated as described previously (16). After isolation, cells were split twice to increase the cell number and all experiments were performed at passage 2. Sixteen hours before labeling, differentiation medium was changed to pre-labeling medium (DMEM, 1 g/liter of glucose, 10 mM HEPES, 10% FBS). Cells were incubated for 3 h with 1 ml of labeling media (DMEM, 10 mM HEPES, 1 g/liter of glucose, 0.25% FA-free BSA, 1 mM carnitine) containing 500 μM [1-^{14}C]oleic acid. To distinguish between the oxidation of endogenous and exogenous FA pools, a pulse-chase experiment was performed. Differentiated primary brown adipocytes (in 12-well plates) from control and *Gpat4$^{-/-}$* neonates were labeled with 500 μM [9,10-^{3}H]oleate for 1.5 h, and the medium was removed. To measure total oxidation, fresh medium containing 500 μM [9,10-^{3}H]oleate was added for an additional 1.5 h, and [^{3}H]H_2O was counted. To measure endogenous oxidation, a second group of dishes containing differentiated primary brown adipocytes was labeled with 500 μM [9,10-^{3}H]oleate for 1.5 h, and the specific activity of the stored TAG was calculated from the amounts of [^{3}H]TAG and total TAG present. Dishes from this set of labeled cells were then incubated for an additional 1.5 h with medium containing 500 μM unlabeled oleate, and [^{3}H]H_2O was counted. In these dishes, any label present would have originated from stored labeled fatty acid. Exogenous oxidation was calculated by subtracting endogenous oxidation from total oxidation.

Radioactive oxidation metabolites in the medium were extracted and measured as described above. Cells were washed with pre-warmed PBS containing 1% BSA before lipids were extracted (13). Lipid extracts and standards were separated by thin layer chromatography on Partisil LK5D Silica gel plates in a two-phase system: chloroform:methanol:ammonium hydroxide (65:25:4, v/v/v) run to 50% of the plate, then air dried and run in heptane:isopropyl ether:acetic acid (60:40:4) to the top of the plate. Authentic lipid standards were visualized by iodine staining. ^{14}C-Labeled lipids were quantified with a Bioscan AR-2000 Imaging Scanner. ^{3}H-Labeled lipids were scraped from thin layer chromatography plates, transferred to scintillation vials, and counted.

Statistics—Data represent mean ± S.E. of at least three independent experiments performed in triplicate unless otherwise indicated. *In vitro* models were analyzed by Student's *t* test comparing each genotype to controls. *In vivo* models were analyzed by two-way analysis of variance and post hoc comparisons of diet conditions within each genotype. Data were considered significant with $p < 0.05$.

Results

When Dietary Fat Was the Major Macronutrient, Growth and Weight Gain in Gpat4$^{-/-}$ Mice Were Impaired— *Gpat4$^{-/-}$* mice were a normal size at birth, but in contrast to the phenotype of mouse pups lacking GPAT1 (2) or GPAT3 (4), at weaning they were smaller than their littermates; by postnatal day 21, *Gpat4$^{-/-}$* weanling mice had gained 25% less weight than controls and were 10% shorter (Fig. 1, *A* and *B*). Between the second and the fifth week of life, the growth rate of the *Gpat4$^{-/-}$* mice was slower than that of their littermates, but by 6 weeks of age the growth rates were similar (Fig. 1*C*). Similar results were observed in female mice (data not shown). Because adult female mice lacking GPAT4 are protected from diet-induced obesity (7), we wondered whether the growth lag during the suckling period was due to the composition of mouse milk, in which TAG comprises 40 to 55% of total caloric energy (17). To characterize an energy defect specifically associated with high dietary fat, control and *Gpat4$^{-/-}$* mice were fed either a 10% fat (LFD) or 45% fat diet (HFD) for 8 weeks. Weight gain was similar in genotypes fed the LFD. When fed the HFD, control mice became obese and accumulated 3-fold more inguinal adipose tissue (Fig. 1, *D* and *E*). In contrast, *Gpat4$^{-/-}$* male mice remained lean, and inguinal adipose mass was similar regardless of diet. The lack of adipose tissue accumulation in *Gpat4$^{-/-}$* mice was not due to a defect in TAG synthesis, because GPAT specific activity in inguinal adipose was identical in both genotypes (Fig. 1*F*). Representative photos illustrate the differences in body size at birth, p17, p28, and 8 weeks of age, and after 8 weeks of consuming the HFD (Fig. 1*G*). These data suggest that mice lacking GPAT4 grow poorly when fat is the predominant macronutrient in the diet, both during the suckling period and with high fat feeding.

GPAT4-deficient Mice Were Hyper-metabolic with High Fat Feeding—Our data showing that both suckling *Gpat4$^{-/-}$* pups and adults fed a high fat diet are consistent with a previous report that the metabolic rate of adult female *Gpat4$^{-/-}$* mice is 5% higher than controls (7). To determine whether the meta-
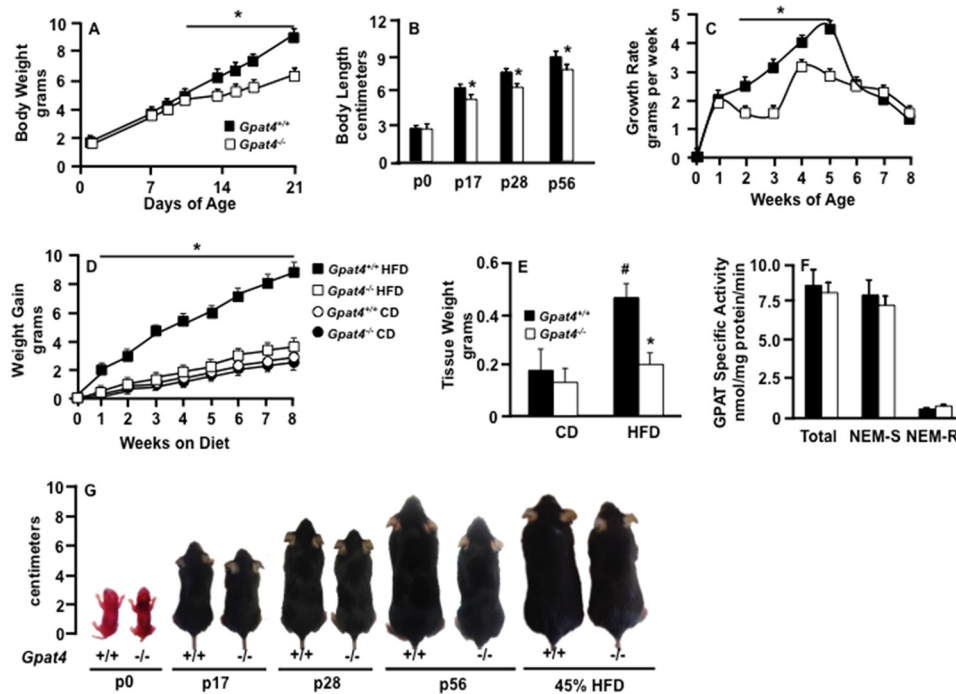
FIGURE 1. **When dietary fat was the predominant dietary macronutrient, $Gpat4^{-/-}$ mice gained less weight and were shorter than controls.** *A–C,* growth and weight gain of control littermate and $Gpat4^{-/-}$ male mice were characterized from birth until 8 weeks of age. *A,* weight gain during suckling. *B,* total body length at birth (p0), postnatal day 17 (*p17*), postnatal day 28 (*p28*), and 8 weeks of age (*p56*). *C,* weekly growth rates of control littermate and $Gpat4^{-/-}$ male mice from birth to 8 weeks of age, $n = 20 - 35$. *D--F,* control and $Gpat4^{-/-}$ male mice were fed a 10% fat (*CD*) or 45% fat diet (*HFD*) for 8 weeks. *D,* weight gain and *E,* inguinal adipose tissue mass, $n = 6$ per genotype, diet. *F,* total, *N*-ethylmaleimide sensitive, and *N*-ethylmaleimide-resistant GPAT specific activity, $n = 6$ per genotype. *G,* representative photographs of control littermate and $Gpat4^{-/-}$ male mice at birth, p17, p28, p56, and after consuming a HFD for 8 weeks (16 weeks old). Data are presented $\pm$ S.E. *, $p < 0.05$, analysis of variance.

bolic rate was higher during high fat feeding, 8-week-old control and $Gpat4^{-/-}$ mice were fed a 45% HFD for 4 weeks. This short-term HFD allowed us to evaluate the metabolic effects of dietary fat content without the confounding variable of obesity. The metabolic rate of $Gpat4^{-/-}$ mice fed the HFD was 12% higher than that of controls, with the major difference occurring primarily during the light cycle (Fig. 2*A*). Food consumption and physical activity were similar between genotypes (Fig. 2, *B* and *C*). These findings suggest that the metabolic rate was accelerated in fat-fed $Gpat4^{-/-}$ mice.

In the Absence of GPAT4, the Absorption of Dietary TAG Was Not Impaired—It has been estimated that monoacylglycerol acyltransferase in intestinal epithelial cells is responsible for 75% of dietary TAG absorption (18). Although GPAT activity is responsible for the remaining 25%, it is not able to rescue the deficit in fat absorption when monoacylglycerol acyltransferase-2 is absent (18). To determine the importance of intestinal GPAT4 and whether its loss might play a role in the lack of weight gain of high fat-fed $Gpat4^{-/-}$ mice, GPAT activity was measured in intestinal mucosa from duodenum, upper and lower jejunum, and ileum. Compared with control duodenum and upper jejunum, total GPAT-specific activities of $Gpat4^{-/-}$ mice were 90 and 40% lower, respectively (Fig. 2*D*). In the lower jejunum, total GPAT specific activity was similar in both genotypes, but in the ileum, the total GPAT specific activity of $Gpat4^{-/-}$ mice was 42% higher than that of controls, suggesting overcompensation by another GPAT isoform. Because duodenal GPAT activity in $Gpat4^{-/-}$ mice was 90% lower than controls, we wondered whether malabsorption of dietary fat

might have reduced weight gain in these mice. However, during the 6 h after an oral fat tolerance test, the amount of TAG accumulation in plasma did not differ between genotypes, showing that the immediate absorption of dietary TAG in $Gpat4^{-/-}$ mice was not delayed (Fig. 2*E*). To assess the impact of GPAT4 deficiency on fat absorption over a longer period of time, mice were housed individually and fed a 60% fat diet for 1 week. The amount of fecal TAG was similarly low in both genotypes, consistent with normal TAG absorption (Fig. 2*F*), and lipid staining in the intestinal mucosa was also similar in both genotypes, showing that dietary TAG had not accumulated without being absorbed (Fig. 2*G*). Taken together, these data confirm that, despite severely depleted GPAT activity in the upper intestine of $Gpat4^{-/-}$ mice, TAG absorption remained normal. It appears then, either that the activity of intestinal monoacylglycerol acyltransferase is sufficient for normal fat absorption or, less likely, that the up-regulated GPAT activity in the ileum is sufficient to compensate for deficient absorption by the proximal intestine (18).

The Increased Metabolic Rate of Gpat4$^{-/-}$ Mice Did Not Occur to Maintain Body Temperature—Consistent with an increase in metabolic rate that is unrelated to increased heat loss, the daytime temperature of $Gpat4^{-/-}$ female mice fed a HFD was 1 ºC higher than controls (Fig. 3*A*). In another test to determine whether reliance on fatty acids for fuel would alter body temperature, mice were fasted for 24 h. Similar to the results of the HFD, the body temperature of $Gpat4^{-/-}$ mice was ~2 °C higher than controls (Fig. 3*B*). To determine whether the previously reported lack of subdermal adipose tissue in
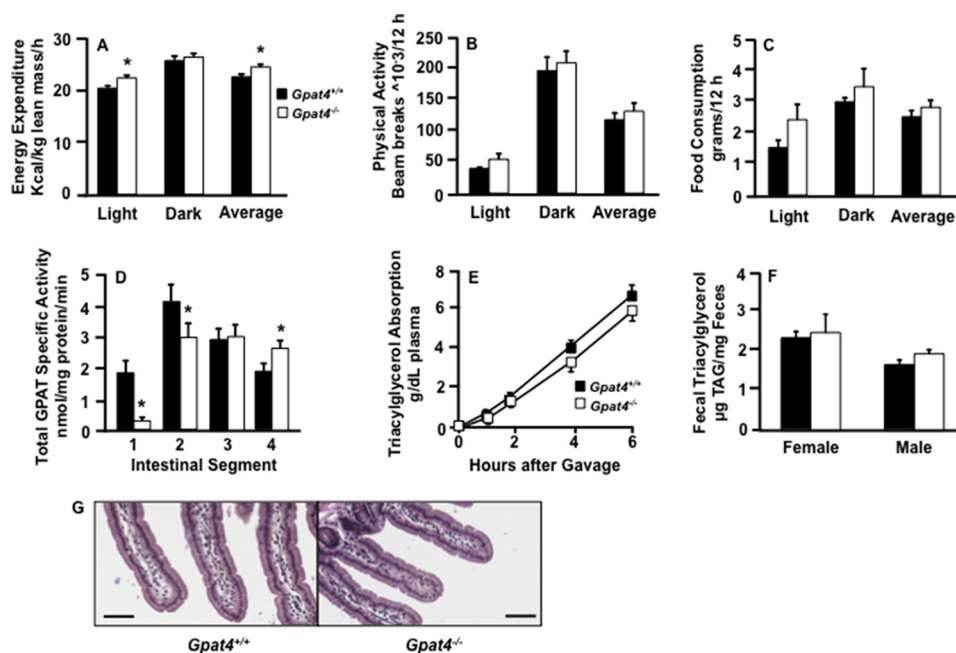
FIGURE 2. **Gpat4$^{-/-}$ mice were hypermetabolic when fed a high fat diet.** *A–C,* energy expenditure, physical activity, and food consumption in female control and *Gpat4*$^{-/-}$ mice fed a 45% fat diet for 4 weeks, $n = 6$. *D,* total membrane preparations were obtained from littermate control and *Gpat4*$^{-/-}$ female mice fed a 10% fat diet for 4 weeks. GPAT specific activities in four equal sections of the small intestine. *E,* female control and *Gpat4*$^{-/-}$ mice fed a 10% fat diet for 4 weeks, then gavaged with 200 μl of olive oil. Fifteen min before gavage, 500 mg/kg of Tyloxapol was injected into the retroorbital plexus. Blood was collected at 0, 1, 2, 4, and 6 h after gavage and plasma TAG were measured; $n = 5$. *F,* fecal TAG content of littermate control and *Gpat4*$^{-/-}$ mice of both sexes. Mice were individually housed and fed a diet containing 60 kcal from fat for 7 days, $n = 5$. *G,* representative images of jejunum from control and *Gpat4*$^{-/-}$ female mice fed a 45% HFD. Tissue was fixed in 1.5% glutaraldehyde, stained with 2% osmium tetroxide, and visualized by light microscopy, $n = 4$; $\times$20 magnification, *scale bars* = 100 μm. Data are presented $\pm$ S.E. *, $p < 0.05$, analysis of variance.
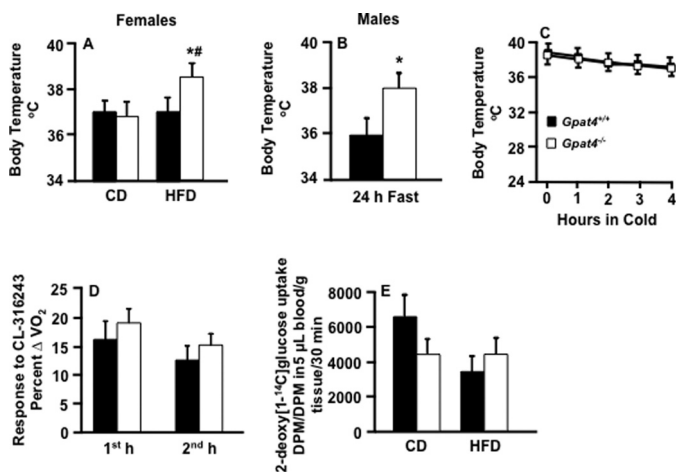

FIGURE 3. **GPAT4-deficient mice release excess heat without constitutive heat loss.** *A,* daytime body temperature of female *Gpat4*$^{-/-}$ mice fed a 10% fat (*CD,* 10% fat diet) or 45% fat diet (HFD) for 4 weeks. Rectal temperature was measured between 10 a.m. and 12 p.m., $n = 6$ per diet/genotype. *B,* body temperature of control and *Gpat4*$^{-/-}$ male mice fasted for 24 h. Rectal temperature was measured between 10 a.m. and 12 p.m. (day), $n = 6$–10. *C,* body temperature of fasted control and *Gpat4*$^{-/-}$ female mice exposed to 4 °C for 4 h, $n = 5$. *D,* oxygen consumption rate in control and *Gpat4*$^{-/-}$ female mice after injection of CL-316243 (5 mg/kg), $n = 5$. *E,* 2-deoxy[1-^{14}C]glucose uptake in BAT from control and *Gpat4*$^{-/-}$ female mice fed a 10 or 45% fat diet for 4 weeks, $n = 5$–6. Data are normalized to tissue weight and radioactive counts in 5 μl of plasma for 5 min after intraperitoneal injection. Data are presented $\pm$ S.E. *, $p < 0.05$ genotype; #, $p < 0.05$ diet, analysis of variance.

Gpat4$^{-/-}$ mice (5) eliminates a necessary insulating layer, 12-week-old control and *Gpat4*$^{-/-}$ mice were challenged with a cold tolerance test. Body temperatures during the challenge were similar between genotypes, suggesting that the insulating subcutaneous fat layer in *Gpat4*$^{-/-}$ mice was sufficient to pre-

vent excessive heat loss (Fig. 3*C*). In addition, GPAT4 contributes minimally to total GPAT activity in white adipose tissue (Fig. 1*F*) (1). Maintenance of body temperature during cold exposure relies on an ability of the animal to minimize heat loss and generate sufficient heat by shivering and BAT-mediated thermogenesis (19). Because BAT is modifiable in rodents, extended periods of exposure to temperatures below thermoneutrality ($\sim$30 °C) increase the thermogenic capacity of BAT. To test thermogenic capacity, we measured the oxygen consumption rate after intraperitoneal injection of the β3-adrenergic agonist, CL316243. If the lack of subdermal adipose tissue were causing excessive heat loss, *Gpat4*$^{-/-}$ mice would increase oxygen consumption more than controls. During the first hour after treatment with CL316243, the VO$_2$ of both genotypes increased 15–20%, and during the second hour the VO$_2$ remained 13–16% above baseline (Fig. 3*D*). The response to CL316243-stimulated VO$_2$ is consistent with adequate heat retention by *Gpat4*$^{-/-}$ mice. Similarly, the uptake of 2-deoxy[1-^{14}C]glucose into BAT was similar in *Gpat4*$^{-/-}$ mice and controls (Fig. 3*E*). Because glucose uptake into BAT depends on the thermogenic activation of the tissue (20), the finding that glucose uptake was similar suggests an equivalent degree of thermogenesis at room temperature in both genotypes. These responses strongly suggest that the hypermetabolic state of the *Gpat4*$^{-/-}$ mouse is not a response to maintain body temperature.

Despite Normal FA Uptake, Gpat4$^{-/-}$ *BAT Contained Less TAG Than Controls*—Total and NEM-sensitive GPAT activity in *Gpat4*$^{-/-}$ BAT was 65% lower than controls, indicating that GPAT4 is the major GPAT activity in BAT (Fig. 4*A*). *Gpat4*$^{-/-}$
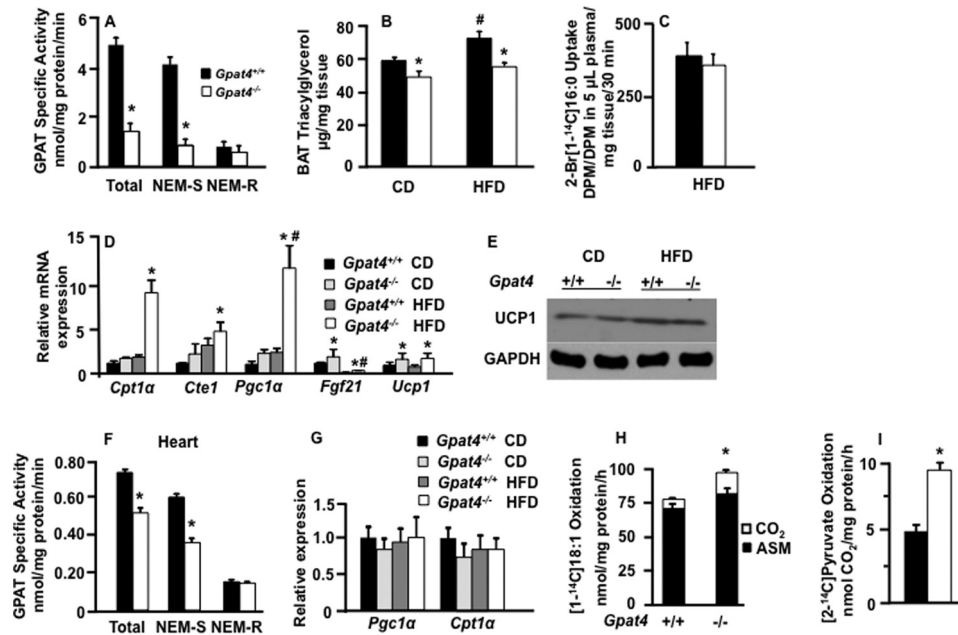
FIGURE 4. **Oxidative capacity was increased in BAT from *Gpat4*$^{-/-}$ mice.** *A–F*, control littermate and *Gpat4*$^{-/-}$ female mice were fed a 10% fat (*CD*) or 45% fat diet (HFD) for 4 weeks. *A*, total, *N*-ethylmaleimide sensitive and *N*-ethylmaleimide-resistant GPAT specific activity in BAT, $n = 6$ per genotype. *B*, BAT triacylglycerol content, $n = 6$ per diet/genotype. *C*, 30 min after retroorbital injection of 2 μCi of 2-Br-[1-^{14}C]palmitate, uptake into BAT was measured, $n = 5$–6. Data are normalized to tissue weight and radioactive counts in 5 μl of plasma collected 5 min after retroorbital injection. *D*, mRNA expression of oxidation-related genes, $n = 6$. Data are normalized to the expression of 36B4. *E*, UCP1 protein levels in tissue lysates. *F*, total, *N*-ethylmaleimide-sensitive and *N*-ethyl-maleimide-resistant GPAT specific activity in heart, $n = 3$ per genotype. *G*, mRNA expression of oxidation-related genes in heart, $n = 3$ per genotype/diet. Data are normalized to GAPDH. *H*, BAT mitochondrial [1-^{14}C]oleic acid oxidation to ASM and carbon dioxide (CO_2). *I*, [2-^{14}C]pyruvic acid oxidation to CO_2, $n = 4$. Data are presented ± S.E. *, $p < .05$ genotype; #, $p < 0.05$ diet, analysis of variance.

BAT from mice fed the LFD contained 17% less TAG than controls (Fig. 4*B*), and BAT from mice fed the HFD contained 25% less TAG than controls. To determine whether FA uptake was reduced in BAT, we measured the uptake of the non-metabolizable 2-Br-[1-^{14}C]palmitate. The uptake of 2-Br-[1-^{14}C]-palmitate into BAT was similar in control and *Gpat4*$^{-/-}$ mice (Fig. 4*C*), indicating that the lack of BAT TAG accumulation in GPAT4-deficient mice did not result from reduced FA uptake.

Thermogenic Gene Expression Increased in BAT from Gpat4$^{-/-}$ *Mice Fed a HFD*—Fatty acids and acyl-CoAs are endogenous ligands for nuclear transcription factors, including PPARs that, when activated, alter cellular energy metabolism (19). Because *Gpat4*$^{-/-}$ BAT contained lower TAG stores but had normal FA uptake, we hypothesized that intracellular FA or acyl-CoAs might influence the expression of PPAR target genes. The expression of the PPARα target genes, *Cpt1α*, *Pgc1α*, *Cte1,* and *Ucp1* was similar in control and *Gpat4*$^{-/-}$ mice fed a low fat diet (Fig. 4*D*), but when *Gpat4*$^{-/-}$ mice were fed a HFD, *Cpt1α*, *Pgc1α*, *Cte1,* and *Ucp1* expression in BAT was 8-, 12-, 1.7-, and 2.5-fold higher, respectively, than in controls (Fig. 4*D*). These diet-induced changes in gene expression suggest that the lack of GPAT4 might increase the intracellular levels of FA or acyl-CoAs in BAT that might then signal to increase PPARα-mediated thermogenesis.

To determine whether lack of GPAT4 increased the expression of PPARα target genes in other tissues, *Pgc1α* and *Cpt1α* were measured in heart tissue. Despite the fact that in *Gpat4*$^{-/-}$ hearts, total and NEM-sensitive GPAT activities were 25 and 33% lower than in controls, respectively (Fig. 4*F*), the expression of PPARα target genes in heart (Fig. 4*G*) and

liver (data not shown) was unaffected in mice fed either diet, suggesting that there might be a threshold for GPAT4 activity whereby activity below this level would result in the up-regulation of PPARα target genes.

Mitochondria from Gpat4$^{-/-}$ *BAT Oxidized More Fatty Acid and Glucose Than Controls*—To determine whether the diet-induced increases in PPARα target gene expression led to increased mitochondrial oxidation, we measured oleate and pyruvate oxidation in BAT mitochondria. Mitochondria from control and *Gpat4*$^{-/-}$ mice fed a HFD were incubated with 200 μM [1-^{14}C]oleate and after 30 min [^{14}C]ASM and [$^{14}CO_2$] were measured. Compared with controls, isolated mitochondria from *Gpat4*$^{-/-}$ BAT oxidized 17 and 200% more oleate to ASM and CO_2, respectively (Fig. 4*H*). Because the amount of [^{14}C]CO_2 was dramatically increased, these data suggested higher TCA cycle flux. To test TCA cycle flux directly, we measured the oxidation of [2-^{14}C]pyruvate. Use of [2-^{14}C]pyruvate permits the measurement of the labeled carbon as released CO_2 after one complete cycle through the TCA cycle. When isolated mitochondria were incubated with 200 μM [2-^{14}C]pyruvate, compared with controls, pyruvate oxidation to CO_2 in *Gpat4*$^{-/-}$ BAT was 2-fold higher (Fig. 4*I*). Thus, when GPAT4 was absent, TCA cycle flux in BAT mitochondria was enhanced.

Adipogenesis Was Normal in Primary Brown Adipocytes from Gpat4$^{-/-}$ *Mice*—Because *in vivo* BAT metabolism is altered by the thermal prehistory of the animal (19), the role of GPAT4 in brown adipose was determined in mature brown adipocytes that had been differentiated from primary *Gpat4*$^{-/-}$ pre-adipocytes. Compared with controls, total GPAT specific activity
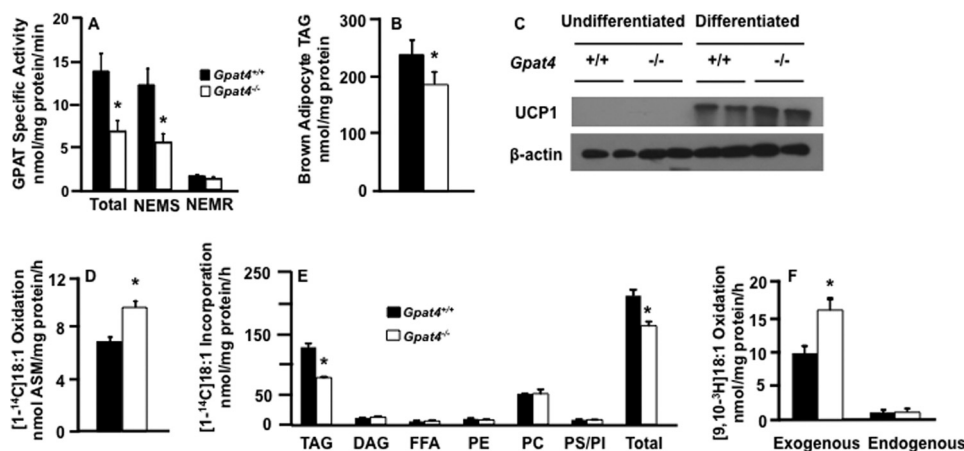
FIGURE 5. **Primary brown adipocytes lacking GPAT4 oxidize 46% more fatty acid than controls.** *A–F*, brown adipocyte precursors isolated from littermate control and *Gpat4*$^{-/-}$ neonates were cultured and differentiated to mature brown adipocytes. *A*, GPAT specific activity and *B*, TAG content, $n = 3–6$. *C*, UCP1 protein levels in undifferentiated and differentiated brown adipocytes. β-Actin used as a loading control. *D* and *E*, differentiated brown preadipocytes from control and *Gpat4*$^{-/-}$ neonates were labeled with 500 μM [1-^{14}C]oleic acid for 3 h. *D*, ASM were extracted from the medium. *E*, cellular lipids were extracted and separated by TLC to quantify [1-^{14}C]oleic acid incorporation into glycerolipids. *F*, differentiated brown adipocytes from control and *Gpat4*$^{-/-}$ neonates were incubated in the presence of 500 μM [9,10-^{3}H]oleic acid for 1.5 h and radioactivity of the medium was immediately measured (total fatty acid oxidation), or the labeling medium was replaced with 500 μM unlabeled oleate for an additional 1.5 h (endogenous fatty acid oxidation). Exogenous fatty acid oxidation rate was calculated by subtracting the endogenous fatty acid oxidation rate from the total fatty acid oxidation rate, $n = 4–6$ animals per genotype in 3 independent experiments. Data are presented $\pm$ S.E. *, $p < 0.05$, Student's *t* test.

in primary adipocytes lacking GPAT4 was 50% lower (Fig. 5*A*). To confirm that differentiation was normal, pre-adipocytes from control and *Gpat4*$^{-/-}$ neonates were cultured in differentiation medium for 0 (preadipocytes) or 7 (adipocytes) days and TAG accumulation and UCP1 expression were determined. In both control and *Gpat4*$^{-/-}$ preadipocytes at day 0, TAG content and UCP1 expression were undetectable (data not shown). Compared with controls, TAG content in differentiated brown adipocytes lacking GPAT4 was 20% lower (Fig. 5*B*), and compared with day 0, the amount of UCP1 protein after 7 days of differentiation was markedly higher, and in *Gpat4*$^{-/-}$ cells appeared modestly higher than controls (Fig. 5*C*). Thus, although GPAT4 is the major GPAT isoform in brown adipocytes, it is not required for normal brown adipocyte differentiation.

GPAT4-deficient Brown Adipocytes Oxidized More Exogenous Fatty Acid Than Controls—Because GPAT initiates the esterification pathway of complex lipid synthesis, we hypothesized that GPAT4-deficient brown adipocytes would esterify less acyl-CoA, thereby allowing more acyl-CoAs to be oxidized. To test this hypothesis, control and *Gpat4*$^{-/-}$ cells were incubated for 3 h with [1-^{14}C]oleate. Brown adipocytes lacking GPAT4 incorporated oleate into TAG at a 33% lower rate than controls, and oxidized oleate at a 40% higher rate (Fig. 5, *D* and *E*). The incorporation of [1-^{14}C]oleate into diacylglycerol and phospholipids was similar in cells from each genotype. These results suggest that when high amounts of FA enter BAT, GPAT4 would normally divert the FA away from β-oxidation and toward esterification into TAG.

Adding exogenous oleate to the culture medium of brown adipocytes stimulates thermogenesis and FA oxidation (12). To distinguish between the oxidation of endogenous and exogenous FA pools, a pulse-chase experiment was performed. Differentiated primary brown adipocytes from control and *Gpat4*$^{-/-}$ neonates were labeled with [9,10-^{3}H]oleate for 1.5 h. To measure total oxidation, the medium was removed, fresh

medium containing [9,10-^{3}H]oleate was added for an additional 1.5 h, and [^{3}H]H$_2$O was counted. To measure endogenous oxidation, cells were labeled with [9,10-^{3}H]oleate for 1.5 h, medium was removed, and the specific activity of the stored TAG was calculated from the amount of [^{3}H]TAG and total TAG present in the cells. The labeled cells were then incubated with medium containing unlabeled oleate for 1.5 h and [^{3}H]H$_2$O was counted. Exogenous oxidation was calculated by subtracting endogenous oxidation from total oxidation. Total oleate oxidation in *Gpat4*$^{-/-}$ brown adipocytes was 33% higher than controls (Fig. 5*F*). In both control and *Gpat4*$^{-/-}$ cells, more than 90% of the total oleate oxidized originated exogenously and, compared with controls, *Gpat4*$^{-/-}$ brown adipocytes oxidized exogenous oleate at a rate that was 45% higher (Fig. 5*F*). The remaining 10% of oxidized oleate originated from endogenous TAG stores and was oxidized at a similar rate by both genotypes. These results indicate that when brown adipocytes are exposed to a high oleate concentration, they primarily oxidize the exogenous oleate. Because more oleate was oxidized by *Gpat4*$^{-/-}$ cells, it appears that the role of GPAT4 in BAT is to promote oleate storage as TAG and to diminish the availability of exogenous oleate for β-oxidation.

Discussion

The initial report describing *Gpat4*$^{-/-}$ mice suggested that they were protected from diet and genetically induced obesity, and that their higher metabolic rate at 2 months resulted from an inadequate insulating subdermal adipose tissue layer (5). The higher metabolic rate of *Gpat4*$^{-/-}$ mice was attributed to increased adaptive thermogenesis in BAT. Because subdermal adipose tissue is minimally present until 2 months of age (5), any absence of subdermal adipose in *Gpat4*$^{-/-}$ mice would not explain impaired growth during the suckling period. Our findings suggest a different interpretation: that the increased metabolic rate resulted from the uncontrolled oxidation of excess exogenous FA by brown adipocytes. Supporting this interpre-

tation are data showing that $Gpat4^{-/-}$ female mice fed a HFD for 4 weeks had a metabolic rate that was 12% higher and core body temperature 1 °C higher than controls. The higher metabolic rate and body temperature that occurs in $Gpat4^{-/-}$ mice is inconsistent with adaptive thermogenesis, which is designed to maintain normal body temperature. In addition, mice lacking GPAT4 displayed normal cold tolerance, and they reacted normally to the β3-adrenergic agonist CL316243. Taken together, these data indicate that the hypermetabolic state of $Gpat4^{-/-}$ mice is not a response to chronic heat loss.

BAT thermogenesis is activated by cold exposure, β-adrenergic stimulation, and FA in a UCP1-dependent manner (21, 22). UCP1 is a gated pore that, when activated, permits the transport of protons across the inner mitochondrial membrane, thereby uncoupling the electron transport from ATP production (23). Active BAT replenishes its intracellular lipid stores via uptake of FA from plasma (24, 25). Our data suggest that GPAT4 is not only responsible for maintaining BAT TAG stores, but also for regulating the use of FAs by BAT.

In addition to their metabolic roles in energy metabolism, FAs and acyl-CoAs derived from exogenous FAs or from the lipolysis of endogenous pools of TAG, act as ligands for the PPAR family of nuclear transcription factors, which have broad effects on cellular energy metabolism (26). In HFD-fed $Gpat4^{-/-}$ mice, the increased mRNA abundance in BAT of the PPARα target genes, $Cpt1\alpha$, $Pgc1\alpha$, $Cte1$, and $Ucp1$, and the increased rate of oleate oxidation suggests an exogenous source of PPAR ligands. Lack of GPAT4, an enzyme present on the endoplasmic reticulum that is responsible for 65% of the initial esterification of glycerol-3-P in BAT, might be expected to markedly diminish the rate of glycerolipid synthesis and allow more acyl-CoAs to enter the mitochondrial matrix for β-oxidation. Additionally, because exogenous FAs entering brown adipocytes are effective PPARα ligands (27), the diminished capacity for FA esterification would allow FAs to be diverted to signaling pathways. This interpretation is supported by data showing that GPAT4$^{-/-}$ primary brown adipocytes oxidized exogenous, but not endogenous, oleate at a higher rate than controls; thus, the lipid signals in $Gpat4^{-/-}$ BAT were probably either exogenous FAs or metabolites derived from FA oxidation.

When the thermogenic effects of norepinephrine are blocked by the β-adrenergic receptor antagonist, propranolol, thermogenesis in brown fat cells can be stimulated by exogenous oleate (21), suggesting that exogenous FA can be oxidized independently of lipolytic stimuli. Consistent with these observations, when primary brown adipocytes were incubated with [^{3}H]oleate, ~90% of the oxidized FA originated exogenously. TAG turnover in working hearts is similar (28); the entry of high amounts of exogenous FA diminishes the use of stored TAG for energy. Because the lack of GPAT4 in brown adipocytes resulted in a 45% higher rate of exogenous FA oxidation than in control cells, GPAT4 appears to limit FA availability for FA-induced thermogenesis. Importantly, in GPAT4-deficient primary hepatocytes, oxidation of exogenously derived FA is normal (29), suggesting that the mechanism whereby GPAT4 limits exogenous FA oxidation is specific to BAT and likely involves the FA-activated protein, UCP1.

In brown adipocytes, maximal thermogenesis can be stimulated independently by oleate and norepinephrine, but co-treatment is not synergistic (21), suggesting that FA-induced thermogenesis and cold-activated thermogenesis occurs through the same mechanism. Although limiting cold-activated thermogenesis would be counterproductive, preventing the occurrence of thermogenesis induced by the presence of excess exogenous FAs would ensure optimal metabolic efficiency. The abnormal thermogenesis that occurred with high fat feeding resulted in poor growth during the suckling period and a hypermetabolic phenotype in adults. These consequences suggest that in BAT GPAT4 normally limits the oxidation of exogenous FAs, particularly when increased thermogenesis would be inappropriate. Most studies find that high fat feeding increases $Ucp1$ mRNA and protein content, although the magnitude of the increases are variable and do not correlate with either the percent of dietary fat or the duration of the fat feeding (30). The idea that excess calories might provoke an increase in BAT-mediated energy wasting has seemed unlikely in an evolutionary sense, and the variability of the effect does not support it as a major feature of fat feeding. However, the findings that $Gpat4^{-/-}$ pups consuming high fat milk grow poorly and that adult $Gpat4^{-/-}$ mice fed a HFD are hypermetabolic strongly suggest that, in the absence of cold exposure, GPAT4 is required to limit excessive oxidation of exogenous FAs. When this limitation is absent, FA-induced thermogenesis induces a hypermetabolic state that is detrimental to the animal.

References

1. Neschen, S., Morino, K., Hammond, L. E., Zhang, D., Liu, Z. X., Romanelli, A. J., Cline, G. W., Pongratz, R. L., Zhang, X. M., Choi, C. S., Coleman, R. A., and Shulman, G. I. (2005) Prevention of hepatic steatosis and hepatic insulin resistance in mitochondrial acyl-CoA:glycerol-sn-3-phosphate acyltransferase 1 knock out mice. *Cell Metab.* **2,** 55–65

2. Hammond, L. E., Gallagher, P. A., Wang, S., Posey-Marcos, E., Hiller, S., Kluckman, K. D., Posey-Marcos, E. L., Maeda, N., and Coleman, R. A. (2002) Mitochondrial glycerol-3-phosphate acyltransferase-deficient mice have reduced weight and liver triacylglycerol content and altered glycerolipid fatty acid composition. *Mol. Cell. Biol.* **22,** 8204–8214

3. Ellis, J. M., Paul, D. S., Depetrillo, M. A., Singh, B. P., Malarkey, D. E., and Coleman, R. A. (2012) Mice deficient in glycerol-3-phosphate acyltransferase-1 have a reduced susceptibility to liver cancer. *Toxicol. Pathol.* **40,** 513–521

4. Cao, J., Perez, S., Goodwin, B., Lin, Q., Peng, H., Qadri, A., Zhou, Y., Clark, R. W., Perreault, M., Tobin, J. F., and Gimeno, R. E. (2014) Mice deleted for GPAT3 have reduced GPAT activity in white adipose tissue and altered energy and cholesterol homeostasis in diet-induced obesity. *Am. J. Physiol. Endocrinol. Metab.* **306,** E1176–E1187

5. Cao, J., Li, J. L., Li, D., Tobin, J. F., and Gimeno, R. E. (2006) Molecular identification of microsomal acyl-CoA:glycerol-3-phosphate acyltransferase, a key enzyme in de novo triacylglycerol synthesis. *Proc. Natl. Acad. Sci. U.S.A.* **103,** 19695–19700

6. Cattaneo, E. R., Pellon-Maison, M., Rabassa, M. E., Lacunza, E., Coleman, R. A., and Gonzalez-Baro, M. R. (2012) Glycerol-3-phosphate acyltransferase-2 is expressed in spermatic germ cells and incorporates arachidonic

acid into triacylglycerols. *PloS One* **7,** e42986

7. Vergnes, L., Beigneux, A. P., Davis, R., Watkins, S. M., Young, S. G., and Reue, K. (2006) Agpat6 deficiency causes subdermal lipodystrophy and resistance to obesity. *J. Lipid Res.* **47,** 745–754

8. Nagle, C. A., Vergnes, L., Dejong, H., Wang, S., Lewin, T. M., Reue, K., and Coleman, R. A. (2008) Identification of a novel *sn*-glycerol-3-phosphate acyltransferase isoform, GPAT4 as the enzyme deficient in Agpat6$^{-/-}$ mice. *J. Lipid Res.* **49,** 823–831

9. Beigneux, A. P., Vergnes, L., Qiao, X., Quatela, S., Davis, R., Watkins, S. M., Coleman, R. A., Walzem, R. L., Philips, M., Reue, K., and Young, S. G. (2006) Agpat6: a novel lipid biosynthetic gene required for triacylglycerol production in mammary epithelium. *J. Lipid Res.* **47,** 734–744

10. Zhang, C., Cooper, D. E., Grevengoed, T. J., Li, L. O., Klett, E. L., Eaton, J. M., Harris, T. E., and Coleman, R. A. (2014) Glycerol-3-phosphate acyltransferase-4-deficient mice are protected from diet-induced insulin resistance by the enhanced association of mTOR and rictor. *Am. J. Physiol. Endocrinol. Metab.* **307,** E305–E315

11. Lewin, T. M., Schwerbrock, N. M., Lee, D. P., and Coleman, R. A. (2004) Identification of a new glycerol-3-phosphate acyltransferase isoenzyme, mtGPAT2, in mitochondria. *J. Biol. Chem.* **279,** 13488–13495

12. Drover, V. A., Ajmal, M., Nassir, F., Davidson, N. O., Nauli, A. M., Sahoo, D., Tso, P., and Abumrad, N. A. (2005) CD36 deficiency impairs intestinal lipid secretion and clearance of chylomicrons from the blood. *J. Clin. Invest.* **115,** 1290–1297

13. Folch, J., Lees, M., and Sloane Stanley, G. H. (1957) A simple method for the isolation and purification of total lipides from animal tissues. *J. Biol. Chem.* **226,** 497–509

14. Buhman, K. K., Smith, S. J., Stone, S. J., Repa, J. J., Wong, J. S., Knapp, F. F., Jr., Burri, B. J., Hamilton, R. L., Abumrad, N. A., and Farese, R. V., Jr. (2002) DGAT1 is not essential for intestinal triacylglycerol absorption or chylomicron synthesis. *J. Biol. Chem.* **277,** 25474–25479

15. Ellis, J. M., Li, L. O., Wu, P. C., Koves, T. R., Ilkayeva, O., Stevens, R. D., Watkins, S. M., Muoio, D. M., and Coleman, R. A. (2010) Adipose acyl-CoA synthetase-1 directs fatty acids toward beta-oxidation and is required for cold thermogenesis. *Cell Metab.* **12,** 53–64

16. Irie, Y., Asano, A., Cañas, X., Nikami, H., Aizawa, S., and Saito, M. (1999) Immortal brown adipocytes from p53-knockout mice: differentiation and expression of uncoupling proteins. *Biochem. Biophys. Res. Commun.* **255,** 221–225

17. Aoki, N., Yamaguchi, Y., Ohira, S., and Matsuda, T. (1999) High fat feeding of lactating mice causing a drastic reduction in fat and energy content in milk without affecting the apparent growth of their pups and the production of major milk fat globule membrane components MFG-E8 and butyrophilin. *Biosci. Biotechnol. Biochem.* **63,** 1749–1755

18. Yen, C. L., Cheong, M. L., Grueter, C., Zhou, P., Moriwaki, J., Wong, J. S., Hubbard, B., Marmor, S., and Farese, R. V., Jr. (2009) Deficiency of the intestinal enzyme acyl CoA:monoacylglycerol acyltransferase-2 protects mice from metabolic disorders induced by high-fat feeding. *Nat. Med.* **15,** 442–446

19. Cannon, B., and Nedergaard, J. (2004) Brown adipose tissue: function and physiological significance. *Physiol. Rev.* **84,** 277–359

20. Cannon, B., and Nedergaard, J. (2010) Metabolic consequences of the presence or absence of the thermogenic capacity of brown adipose tissue in mice (and probably in humans). *Int. J. Obes. (Lond)* **34,** S7–S16

21. Lindberg, O., Prusiner, S. B., Cannon, B., Ching, T. M., and Eisenhardt, R. H. (1970) Metabolic control in isolated brown fat cells. *Lipids* **5,** 204–209

22. Matthias, A., Ohlson, K. B., Fredriksson, J. M., Jacobsson, A., Nedergaard, J., and Cannon, B. (2000) Thermogenic responses in brown fat cells are fully UCP1-dependent. UCP2 or UCP3 do not substitute for UCP1 in adrenergically or fatty scid-induced thermogenesis. *J. Biol. Chem.* **275,** 25073–25081

23. Klingenberg, M., Echtay, K. S., Bienengraeber, M., Winkler, E., and Huang, S. G. (1999) Structure-function relationship in UCP1. *Int. J. Obes. Relat. Metab. Disord.* **23,** S24–S29

24. Khedoe, P. P., Hoeke, G., Kooijman, S., Dijk, W., Buijs, J. T., Kersten, S., Havekes, L. M., Hiemstra, P. S., Berbée, J. F., Boon, M. R., and Rensen, P. C. (2015) Brown adipose tissue takes up plasma triglycerides mostly after lipolysis. *J. Lipid Res.* **56,** 51–59

25. Bartelt, A., Bruns, O. T., Reimer, R., Hohenberg, H., Ittrich, H., Peldschus, K., Kaul, M. G., Tromsdorf, U. I, Weller, H., Waurisch, C., Eychmüller, A., Gordts, P. L., Rinninger, F., Bruegelmann, K., Freund, B., Nielsen, P., Merkel, M., and Heeren, J. (2011) Brown adipose tissue activity controls triglyceride clearance. *Nat. Med.* **17,** 200–205

26. Zechner, R., Zimmermann, R., Eichmann, T. O., Kohlwein, S. D., Haemmerle, G., Lass, A., and Madeo, F. (2012) FAT SIGNALS: lipases and lipolysis in lipid metabolism and signaling. *Cell Metab.* **15,** 279–291

27. Mottillo, E. P., Bloch, A. E., Leff, T., and Granneman, J. G. (2012) Lipolytic products activate peroxisome proliferator-activated receptor (PPAR) α and δ in brown adipocytes to match fatty acid oxidation with supply. *J. Biol. Chem.* **287,** 25038–25048

28. Saddik, M., and Lopaschuk, G. D. (1991) Myocardial triglyceride turnover and contribution to energy substrate utilization in isolated working rat hearts. *J. Biol. Chem.* **266,** 8162–8170

29. Wendel, A. A., Cooper, D. E., Ilkayeva, O. R., Muoio, D. M., and Coleman, R. A. (2013) Glycerol-3-phosphate acyltransferase (GPAT)-1, but not GPAT4, incorporates newly synthesized fatty acids into triacylglycerol and diminishes fatty acid oxidation. *J. Biol. Chem.* **288,** 27299–27306

30. Fromme, T., and Klingenspor, M. (2011) Uncoupling protein 1 expression and high-fat diets. *Am. J. Physiol. Regul. Integr. Comp. Physiol.* **300,** R1–R8